



Novel Pyrazole-Linked Pyran Hybrids: Synthesis, Anti-inflammatory Evaluation, Molecular Docking Study

Mohamed A. M. Abdel Reheim¹, Hend S. Abdel Rady¹, Omnia A. Mohamed², Ibrahim S. Abdel Hafiz¹,

Hala M. Reffat¹, Aboubakr H. Abdelmonsef^{3*}

¹Department of Chemistry, Faculty of Science, Arish University, Arish 45511, Egypt

²Department of Biochemistry and Molecular Biology, Theodor Bilharz Research Institute, Giza, Egypt

³Department of Chemistry, Faculty of Science, South Valley University, Qena 83523, Egypt



Abstract

In this study, a series of novel pyrazole-linked pyran hybrids was synthesized starting from 4-acetyl-1,3-diphenyl-1H-pyrazole-5(4H)-one 1. Their structures were characterized by means of spectroscopic techniques. Further, their anti-inflammatory activities were in vitro examined using inhibition of protein denaturation, membrane stabilization assay, and quantitative real-time PCR (qRT-PCR). Compound 6 showed observed anti-inflammatory activity compared with diclofenac. Moreover, the molecular docking approach for the newly prepared hybrid molecules was also performed against phosphodiesterase 4 enzyme (PDE4) to investigate their binding modes of action. Remarkably, compound 6 exhibited the lowest binding energy (-10.8 kcal/mol) against the target. Additionally, the predicted ADMET properties of these molecules exhibited favorable drug-likeness properties.

Keywords: pyrazole-linked pyran; spectroscopic techniques; anti-inflammatory evaluation; PDE4 enzyme; molecular docking.

1. Introduction

Pyrans are heterocyclic scaffolds that are found in various naturally occurring molecules and have remarkable biological activities. They exhibited potential activities as they used in treatment of several disorders. Given its significance as a pharmacophore, Pyran is a key moiety in drug molecules that exhibited anticonvulsant, anti-inflammatory, and antitumor activities [1–4].

On the other hand, pyrazoles have broad spectrum of biological activity like antiviral, antibacterial, anti-inflammatory antidiabetic, and antitumor properties [5–8].

In addition, heterocyclic compounds incorporating pyrazole and pyrane moieties are included in various marketed drugs [9], as represented in **Figure 1**. Combination of pyran with other biologically active scaffolds such as pyrazole in hybrid analogues can lead to identify anti-inflammation inhibitors.

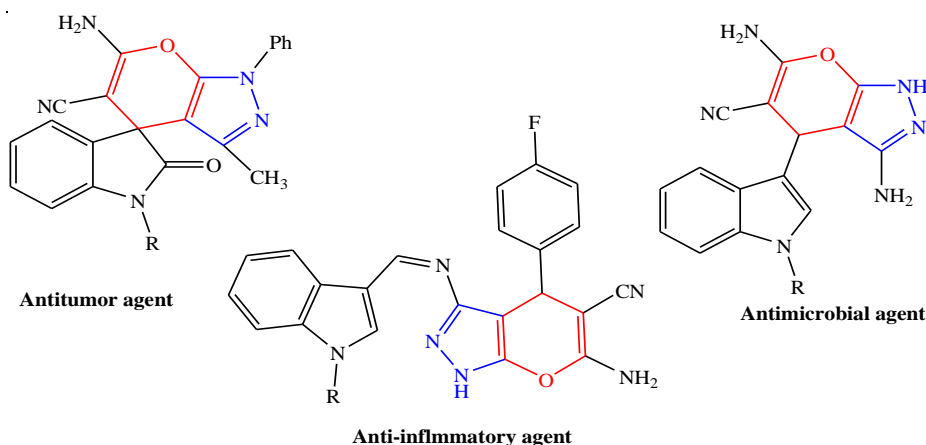


Figure 1. Some drugs with pyran and pyrazole moieties

*Corresponding author e-mail: aboubakr.ahmed@sci.svu.edu.eg; (Aboubakr H. Abdelmonsef).

Receive Date: 20 July 2024, Revise Date: 29 August 2024, Accept Date: 01 September 2024

DOI: 10.21608/ejchem.2024.305934.10053

©2025 National Information and Documentation Center (NIDOC)

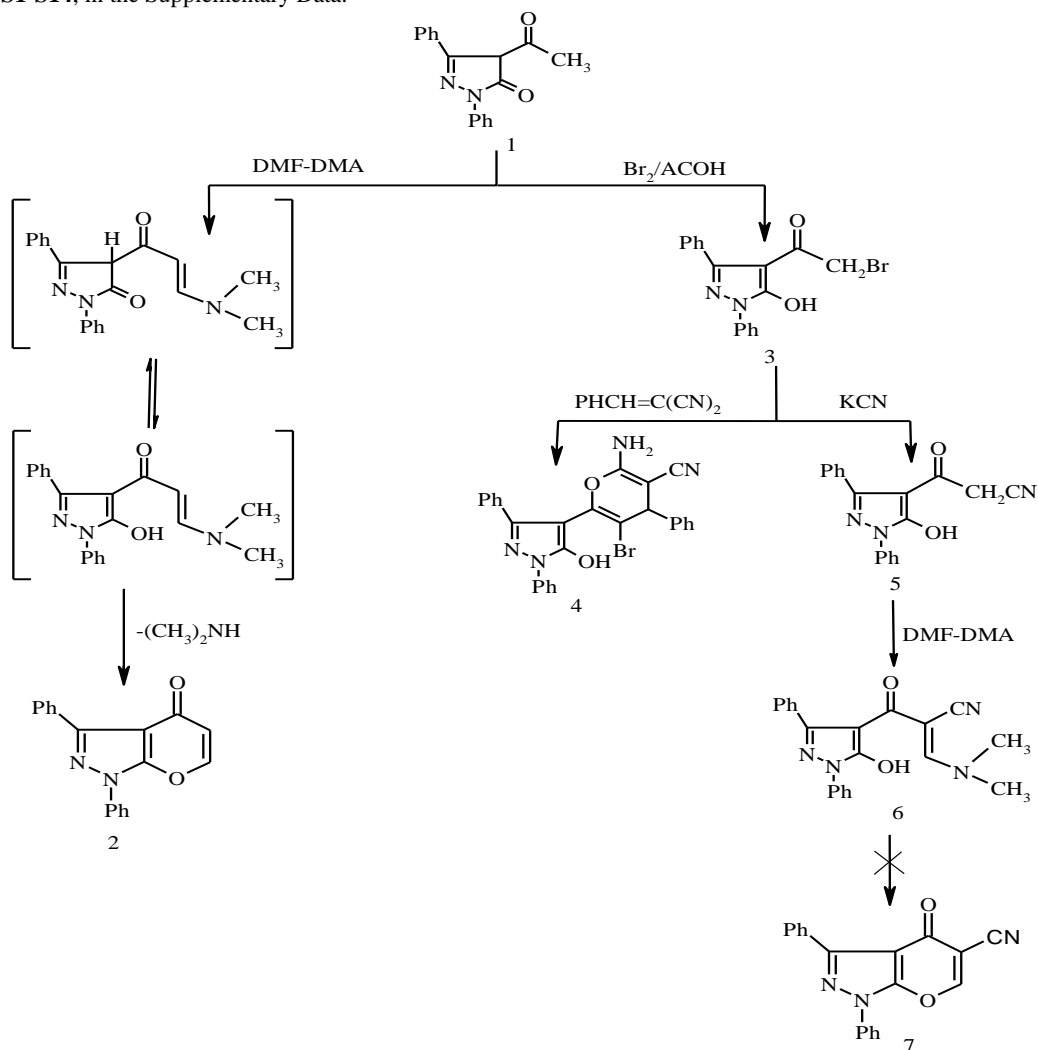
2. Results and discussion

2.1 Chemistry

The synthetic route of newly molecules **2-6** was represented in **Scheme 1**. The pyrano[2,3-c]pyrazol-4(1H)-one derivative **2** was prepared by condensation of compound **1** with DMF-DMA in boiling dioxane. Structure of **2** was mainly elucidated by means of ¹H-NMR spectrum, which revealed signals at δ 7.28-7.30 ppm (d, 1H, =CH), 7.35-7.37 ppm (d, 1H, COCH=), and a multiplet signal at δ 7.49-8.20 ppm corresponding to the aromatic protons. In addition, IR spectrum showed bands for -C=O, -C=N groups. Finally, ¹³C-NMR exhibited signals at δ = 101.93, 115.13, 122.12, 128.55, 129.30, 130.00, 130.55, 131.04, 132.10, 136.15, 146.02, 155.54, 156.15, 177.58

In addition, 2-bromo-1-(5-hydroxy-1,3-diphenyl-1H-pyrazol-4-yl)ethanone **3** was synthesized by bromination of the starting material **1** in acetic acid. Upon undergoing nucleophilic displacement processes, α-bromo carbonyl moiety present in **3** exhibited enhanced reactivity. By treating **3** with arylidene malononitrile and a catalytic quantity of piperidine, 4H-pyran-3-carbonitrile **4** was created in outstanding yield. The active (-CH₂) group in **3** appears to be produced *via* a Michael-type reaction to the activated double bond in arylidene malononitrile, which is subsequently followed by cyclization and tautomerization. Based on analytical and spectroscopic data, structure of **4** was confirmed. IR analysis highlighted -NH₂, CH_{aromatic}, -CN stretching vibrations. In addition, ¹H-NMR spectrum exhibited signals at δ 3.72 (s, 1H, 4H_{pyrane}), 5.36 (s, 2H, NH₂), 7.05-8.17 (m, 15H, Ar-H), 9.30 (s, 1H, OH). Finally, ¹³C-NMR exhibited signals at 38.5, 58.1, 113.1, 113.4, 119.4, 123.0, 126.7, 126.9, 128.1 (s), 128.1, 128.3, 128.6, 137.7, 144.3, 147.9, 150.5, 159.2, 160.3.

Moreover, bromoacetyl pyrazole **3** and potassium cyanide were reacted to form acetonitrile derivative **5**. Additionally, the enaminonitrile derivative **6** was yielded in excellent yield by refluxing compound **5** with DMF-DMA in dry dioxane for approximately 6 hrs, according to Knoevenagel condensation [14]. The structure of **6** was proved using spectral and elemental investigations. Consequently, the signals displayed below were found in ¹H-NMR analysis as a singlet signal at δ 3.58 ppm assigned to -N(CH₃)₂, a singlet signal at δ 5.30 ppm assigned to olefinic proton, multiple signals at δ 7.19-7.91 ppm attributed to Ar-H and a singlet peak at δ 9.80 ppm assigned to hydroxyl group. Moreover, a molecular ion peak at m/z (%) = 358 (M⁺) associated with the chemical formula C₂₁H₁₈N₄O₂ was discovered in the mass spectrum. The obtained data don't support the formation of compound **7**. The spectral data for all synthetic molecules are declared as **Figures S1-S14**, in the Supplementary Data.



Scheme 1. Synthetic route of the newly compounds **2-6**

2.2 In vitro Anti-inflammatory Activity

2.2.1 Inhibition of Protein Denaturation

A comparative analysis was conducted between the synthesized molecules and diclofenac utilizing repeated measures (RM) two-way ANOVA. This analysis revealed a statistically significant interaction between the compounds across various concentrations ($p < 0.0001$). To further delineate the impact of each molecule, multiple t-tests were employed, comparing each concentration with the corresponding concentration of diclofenac. As presented in **Table 1**, the majority of the synthesized molecules exhibited highly significant anti-inflammatory properties. The findings conclusively indicate that all synthesized molecules demonstrated a potent anti-inflammatory effect.

The molecules **3**, **4** and **6** had the highest anti-inflammatory activity followed by **5** then **2** at all concentrations in comparison with the standard drug used; (diclofenac) as shown in **Figure 2**.

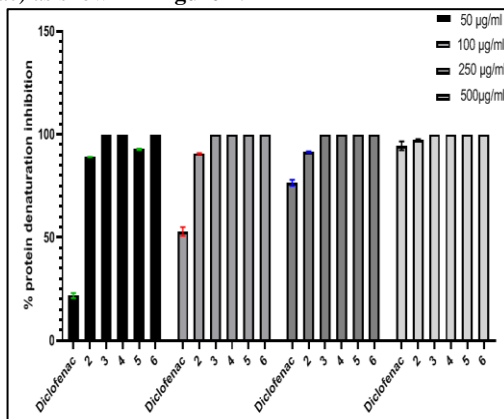


Figure 2. Variation in the percent of protein denaturation inhibition effect of compounds using different concentrations (50, 100, 250 and 500 µg/ml)

Table 1. Analysis of the percent of protein denaturation inhibition of molecules
p value ≤ 0.0001 (very highly significant compared with Diclofenac)

	50 µg/ml	100 µg/ml	250 µg/ml	500 µg/ml
Diclofenac	21.8±1.2	52.9±2.1	76.5±1.5	94.5±2.1
2	89±0.09	90.81±0.19	91.62±0.23	97.56±0.15
3	100±0.06	100±0.3	100±0.33	100±0.28
4	100±0.56	100±0.99	100±0.45	100±0.3
5	92.84±0.35	100±0.04	100±0.94	100±0.19
6	100±0.9	100±0.46	100±0.95	100±0.7

2.2.2 Membrane Stabilization Assay

To assess the statistical interaction between molecules across various concentrations, a repeated measures (RM) two-way ANOVA was employed. The analysis revealed a highly significant effect between the molecules ($p < 0.0001$). Furthermore, multiple t-tests indicated a significant interaction between each molecule and diclofenac. The majority of the molecules demonstrated significant differences, as detailed in **Table 2**. These results suggest that all tested molecules exhibited a notable percentage of protection when compared to diclofenac. The molecules **2** and **3** had the highest protection percent at different concentrations of 50, 100, 250 and 500 µg/ml and The compounds **4**, **5** and **6** had the highest protection present at different concentrations of 50, 100, 250 µg/ml (**Figure 3**).

2.2.3 Quantitative Real-Time PCR Analysis:

The obtained from the Real-Time PCR assay demonstrated a highly statistically significant interaction between the synthesized molecules at varying concentrations, as determined by RM two-way ANOVA ($p < 0.0001$), using beta-actin as the internal control. As indicated in **Table 3**, most molecules exhibited significant differences. Notably, molecule **6** showed the greatest reduction in COX-2 expression levels, followed by Compounds **3** and **4**, particularly at a concentration of 50 µg/ml (**Figure 4**).

Table 2. Analysis of the percent of hemolysis protection of synthesized molecules

	50 µg/ml	100 µg/ml	250 µg/ml	500 µg/ml
Diclofenac	2±0.3	10±0.77	22±0.36	46±0.9
2	100±0.74	100±0.56	100±0.33	100±0.95
3	100±0.09	100±0.89	100±0.01	100±0.08
4	100±0.04	100±0.98	100±0.1	99.89±0.3
5	100±0.78	100±0.79	100±0.09	99.97±0.44
6	100±0.54	100±0.05	100±0.88	99.87±0.66

p value ≤ 0.0001 was a very highly significant compared to Diclofenac.

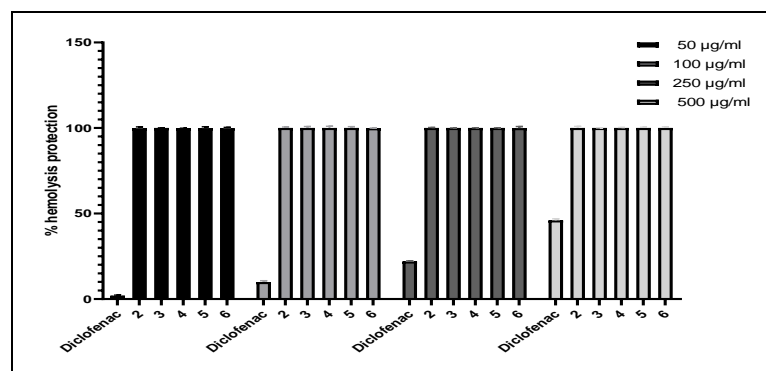


Figure 3. The graph represents the variation in the protection percent from hemolysis of molecules with different concentrations (50, 100, 250 and 500 µg/ml)

Table 3. Analysis of the effect of molecule at concentration 50 µg/ml on COX-2 expression level

	Untreated CT	Untreated ($2^{-\Delta Ct}$)	3 CT	3 ($2^{-\Delta Ct}$)	4 CT	4 ($2^{-\Delta Ct}$)	6 CT	6 ($2^{-\Delta Ct}$)
Beta- actin	35.94	—	40.65	—	44.79	—	36.9	—
cox2	32.89	1	33.27	0.04972	34.9	0.0087	30	14.42001

p value ≤ 0.0001 was a very highly significant compared to reference drug.

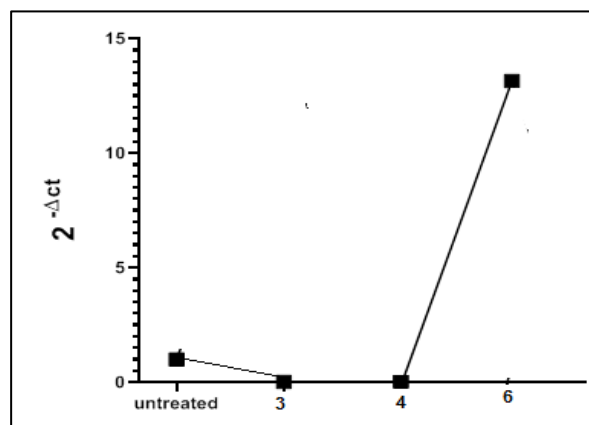


Figure 4. The graph represents the variation in the level of COX-2 expression affected by molecules using concentration 50 µg/ml

2.3 Molecular docking technique and ADMET analysis

In order to investigate how molecules docked to binding regions of the target, molecular docking approach was achieved against PDE4 enzyme (PDB ID: 3ly2), as represented in **Figure 5**. Phosphodiesterase 4 enzyme (PDE4) is selected as a target for identification of anti-inflammatory agents because it is expressed in many anti-inflammatory cells [15]. The compounds were successfully docked to the enzyme through hydrogen bonds and arene-stacked interactions. The 2D and 3D docking pose images of docked compounds with the enzyme are declared in **Figure 5**. The 2D structures, binding energies Kcal/mol, docked residues and distances (Å) are tabulated in **Table 4**.

Compound **2** docked to the target through two H-bonds and three arene-arene and one arene-sigma interactions with the residues Tyr233, Gln443, Phe446, Phe414 and Ile410, respectively. Compound **3** exhibited two H-bonds and two arene-arene interactions with Tyr233, and Phe446 at 2.93, 2.33, 4.98, and 4.93 Å respectively. Moreover, molecule **4** showed one H-bond and two arene-arene interactions with Asp392, and Phe446. Compound **5** exhibited only one arene-arene stacking with Phe446. Finally, compound **6** with the best docking score (-10.8 kcal/mol) docked to the target through two H-bonds and one arene-arene interactions with Tyr233, His234 and Phe446 at 2.96, 1.99, and 4.54 Å, respectively.

The drug-likeness of all compounds **2-6** were predicted by using Swiss ADME and AdmetSAR web servers and are tabulated in **Table 5**. M.Wt of all these molecules were in the range of 288.30 – 511.37 g/mol; indicating that they can be easily absorbed. The rotatable bonds in all molecules are ≤ 10 , H-bond donors and acceptors were in accepted range. The topological polar surface (TSPA) of molecules was in the range of 48.03 – 97.09; indicating the acceptable range of results. There are no violations of Lipinski's rule (RO5). The bioavailability score of all compounds is within the prescribed range (0.55); indicating easy absorption in the body. The pharmacokinetic results showed that they have favourable drug-likeness and could be served as potential drug candidates.

Table 4. 2D structures of molecules and their binding energies (Kcal/mol)

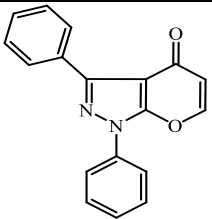
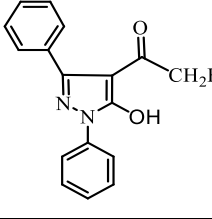
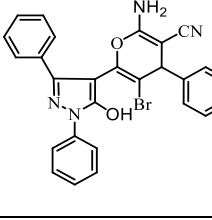
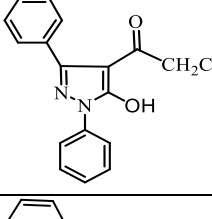
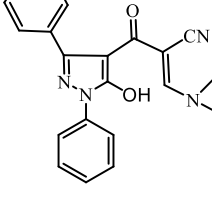
	2D structure	Binding Energy kcal/mol	Docked complex (amino acid–ligand) interactions	Distance (Å)
2		-8.8	H-bonds TYR233:OH-molecule 2 GLN443:NE2-molecule 2 arene-arene interactions PHE446--- molecule 2 PHE446--- molecule 2 PHE414--- molecule 2 arene-sigma interactions ILE410:CG1-molecule 2	2.93 2.95 4.08 4.26 5.38 3.76
3		-8.5	H-bonds TYR233:OH-molecule 3 TYR233:OH-molecule 3 arene-arene interactions PHE446--- molecule 3 PHE446--- molecule 3	2.93 2.33 4.98 4.93
4		-9.6	H-bonds ASP392:OD2-molecule 4 arene-arene interactions PHE446--- molecule 4 PHE446--- molecule 4	2.28 4.28 4.57
5		-8.4	arene-arene interactions PHE446--- molecule 5	4.65
6		-10.8	H-bonds TYR233:OH--- molecule 6 HIS234:NE2--- molecule 6 arene-arene interactions PHE446--- molecule 6	2.96 1.99 4.54

Table 5. ADMET analysis of the molecules 2-6

	Molecular Weight (g/mol)	logp	TPSA A ²	HBA	HBD	N rotatable	N violations	GI absorp tion	Bioavail ability score
Reference range	130-500	<5	≤140	2-20	0-6	≤10	<5		
2	288.30	2.85	48.03	3	0	2	0	High	0.55
3	357.20	2.88	55.12	3	1	4	0	High	0.55
4	511.37	3.41	97.09	4	2	4	1	Low	0.55
5	303.31	1.86	78.91	4	1	4	0	High	0.55
6	358.39	1.66	82.15	4	1	5	0	High	0.55

3. Experimental

3.1 Chemistry

Kofler Block instrument was used to determine the melting points. Using n-hexane and EtOAc, thin layer chromatography (TLC) on aluminium sheets was used to determine the purity of the produced compounds (9:1, V/V, 7:3 V/V) eluent. FTIR 5300 spectrometer (KBr) was used to determine IR spectra (ν , cm^{-1}). Varian Gemini spectrometer was utilized to record the ¹H-NMR (400 MHz) and ¹³C-NMR (100 MHz) spectra, using DMSO-d₆ as solvents. Tetramethylsilane (TMS) was used as an internal reference. 1000 EX mass spectrometer at 70 eV was used to determine the mass spectra. The Microanalytical Research Center, Cairo University, performed the elemental analyses

1,3-diphenylpyrano[2,3-c]pyrazol-4(1H)-one (2): Compound **1** and N-N-dimethylformamide dimethyl acetal were dissolved in dioxane (30 mL) and heated under reflux for 6 hrs. Filtration was used to collect the precipitated solid, which was then dried and recrystallized from EtOH to produce (**2**; 73%) as yellow crystals; m.p.188-190 °C; IR = 3059 (CH_{aromatic}), 1701 (C=O); ¹H-NMR δ = 7.28-7.30 (d, 1H, =CH), 7.35-7.37 (d, 1H, COCH=), 7.49-8.20 (m, 10H, Ar-H); ¹³C-NMR δ = 101.93, 115.13, 122.12, 128.55, 129.30, 130.00, 130.55, 131.04, 132.10, 136.15, 146.02, 155.54, 156.15, 177.58; MS= *m/z* (%) 288 (M⁺). Anal. calcd. For C₁₈H₁₂N₂O₂ (288): C, 74.99; H, 4.20; N, 9.72; Found: C, 74.13; H, 4.25; N, 9.79%.

2-bromo-1-(5-hydroxy-1,3-diphenyl-1H-pyrazol-4-yl)ethanone (3): Under direct sunlight, bromine was stirred with a solution of **1** (0.01 mol) in acetic acid (10 mL) for 2 hrs. The separated solid was filtered off, cleaned with ethanol and acetic acid, and recrystallized from EtOH to yield (**3**; 73%) as yellow powder; m.p.120-122 °C; IR = 3451 (OH), 3061 (CH_{aromatic}), 1733 (C=O); ¹H-NMR δ = 4.49 (s, 2H, CH₂), 6.68-7.95 (m, 10H, Ar-H), 9.59 (s, 1H, OH); MS= *m/z* (%) 356 (M⁺). Anal. calcd. For C₁₇H₁₃BrN₂O₂ (356): C, 57.16; H, 3.67; N, 7.84; C, 57.24; H, 3.71; N, 7.86%.

2-amino-5-bromo-6-(5-hydroxy-1,3-diphenyl-1H-pyrazol-4-yl)-4-phenyl-4H-pyran-3-carbonitrile (4): For a duration of 24 hrs, a solution comprising 30 mL of ethanol and a catalytic amount of piperidine, compound **3** (0.01 mol) and 2-benzylidene malonitrile was refluxed. After letting the mixture cool, it was poured into a cold diluted HCl. The solid obtained was filtered off, and recrystallized from EtOH to furnish (**4**; 73%) as brown powder; m.p. 233-235 °C; IR = 3449-3400, (OH/ NH₂), 3059 (CH_{aromatic}), 2933 (CH_{aliphatic}), 2193 (CN); ¹H-NMR δ = 3.72 (s, 1H, 4H_{pyrane}), 5.36 (s, 2H, NH₂), 7.05-8.17 (m, 15H, Ar-H), 9.30 (s, 1H, OH); ¹³C-NMR δ = 38.5, 58.1, 113.1, 113.4, 119.4, 123.0, 126.7, 126.9, 128.1 (s), 128.1, 128.3, 128.6, 137.7, 144.3, 147.9, 150.5, 159.2, 160.3; MS= *m/z* (%) 510 (M⁺). Anal. calcd. For C₂₇H₁₉BrN₄O₂ (510): C, 63.42; H, 3.75; N, 10.96; Found: C, 63.49; H, 3.78; N, 10.98%.

3-(5-hydroxy-1,3-diphenyl-1H-pyrazol-4-yl)-3-oxopropanenitrile (5): An aqueous solution KCN (0.01 mol) was mixed to a solution of **3** (0.01 mol) in EtOH (10 mL). After 9 hrs of refluxing, a cold diluted HCl was added to the mixture to cause precipitation. After being filtered, the precipitated solid was dried, cleaned with water, and recrystallized from EtOH to produce (**5**; 73%) as yellow powder; m.p. 188-190 °C; IR = 3451 (OH), 3063 (CH_{aromatic}), 2927 (CH_{aliphatic}), 2233 (CN), 1725 (C=O); ¹H-NMR δ = 4.20 (hump, 2H, CH₂), 6.97-8.10 (m, 10H, Ar-H), 9.30 (s, 1H, OH); MS= *m/z* (%) 303 (M⁺). Anal. calcd. For C₁₈H₁₃N₃O₂ (303): C, 71.31; H, 4.30; N, 13.74; Found: C, 71.35; H, 4.36; N, 13.87%.

3-(dimethylamino)-2-(5-hydroxy-1,3-diphenyl-1H-pyrazol-4-carbonyl)acrylonitrile (6): A mixture of compound **5** and DMF-DMA in dioxane (30 mL) was refluxed for 7 hrs. After that, let it cool. After being separated, the solid was filtered, dried, and recrystallized from EtOH to produce (**6**; 73%) as yellow powder; m.p.178-180 °C; IR = 3445 (OH), 3057 (CH_{aromatic}), 2933 (CH_{aliphatic}), 2246 (CN), 1732 (C=O); ¹H-NMR δ = 3.56 (s, 6H, 2CH₃), 5.30 (s, 1H, CH_{olefinic}), 7.19-7.91 (m, 10H, Ar-H), 9.80 (s, 1H, OH); MS= *m/z* (%) 358 (M⁺). Anal. calcd. For C₂₁H₁₈N₄O₂ (358): C, 70.38; H, 5.06; N, 15.63; Found: C, 70.45; H, 5.08; N, 15.67%.

3.2 In vitro anti-inflammatory assay

3.2.1 Protein denaturation inhibition Assessment:

The anti-inflammatory activity was assessed by inhibiting the denaturation of bovine serum albumin ⁽¹⁰⁾. The reaction mixture included 50 μ l of each test sample at various concentrations (500, 250, 100, and 50 μ g/ml) combined with 450 μ l of a 1% aqueous solution of bovine serum albumin. The pH was adjusted to 6.4 using 1 N HCl. Distilled water served as the negative control, while diclofenac potassium was the reference standard. Samples were incubated at 37°C for 20 minutes,

and then heated to 60°C for 15 minutes. After cooling, turbidity was measured at 600 nm. Each sample was tested in triplicate, with mean values used for calculations. The percentage inhibition of protein denaturation was determined using the equation:

$$\text{Percent of protection} = 100 - (\text{Abs sample}/\text{Abs control})$$

3.2.2 Membrane Stabilization Assay:

The erythrocyte membrane stabilization assay was utilized to evaluate the inflammatory response and anti-inflammatory effects of the synthesized molecules [16]. The reaction mixture comprised an erythrocyte suspension obtained from a healthy human volunteer (who had abstained from NSAIDs for two weeks prior to the experiment) and a hypotonic solution (50 mM NaCl in 10 mM sodium phosphate buffer saline, pH 7.4). Distilled water served as the negative control, while diclofenac sodium was employed as the reference standard at concentrations of 500, 250, 100, and 50 µg/ml. Following incubation at 37°C for 30 minutes, the mixture was centrifuged at 3000 rpm for 20 minutes. The hemoglobin content in the supernatant was then measured at 560 nm. All experiments were conducted in triplicate, with mean values used for calculations. The percentage of RBC membrane stabilization or protection was calculated using the following equation:

$$\text{Percent of protection} = 100 - (\text{Abs sample}/\text{Abs control}).$$

3.2.3 Quantitative Real-Time PCR Analysis:

Peripheral blood mononuclear cells (PBMCs) were isolated from healthy donors who had abstained from NSAIDs for at least four days prior to blood collection. The cells were seeded in a 24-well plate at a density of 1×10^5 cells per 500 µl of culture medium per well. The culture medium consisted of RPMI 1640 (Biowest) supplemented with 10% heat-inactivated fetal bovine serum (FBS) (LONZA), 1% penicillin/streptomycin/fungizone solution (LONZA), and 1% HEPES buffer (1 M). The cells were incubated for 1 hour at 37°C in a 5% CO₂ atmosphere. Following this initial incubation, each test compound was added to the respective wells at a concentration of 50 µg/ml. Diclofenac sodium was used as the reference standard drug, also at a concentration of 50 µg/ml [17]. The plate was then incubated for an additional 24 hours at 37°C in a 5% CO₂ environment.

The cultured PBMC were harvested and RNA extraction was performed using an RNA extraction kit (Biovision, Inc.). Using Novo™ cDNA Kit (Biovision, Inc), SYBR Green master mix (Thermo Fisher Scientific), qPCR was performed. The cycling parameters were: were 95 °C for 10 min followed by 50 cycles of (95 °C denaturation for 20 s, and 55 °C for 30 sec) [18]. StepOne™ Real-Time PCR System (48-well) was used to evaluate the relative expression of the COX₂ gene using cDNA as a template (Thermo fisher scientific, USA), β-actin was used as endogenous control and SYBR Green master mix (Transgen : AQ601-01) using the ΔΔCT method. The following primers sequences were created using NCBI primer design according to Okasha H. et al [19,20] and retrieved from Biovision:

COX2 forward primer: 5'- TGATGATTGCCCGACTCCCT-3'

COX2 Reverse primer 5'- TCATCTGCCTGCTCTGGTCA-3'

β-actin forward primer : 5'- ATCCGCAAAGACCTGTACGC-3'

β-actin Reverse primer : 5'- TCTTCATTGTGCTGGGTGCC -3'

Real time qPCR data were converted to linear data by calculating the 2^{-Ct} values when data are expressed per mg tissue, and by calculating the 2^{-ΔCt} values for COX2 normalized data. Data are expressed as arbitrary units or as ratios of COX-2 expression. Statistical analyses were performed using GraphPad Prism, version 8.00 (GraphPad Software Inc., La Jolla, CA, USA).

3.3 In silico study

The protocols of docking study were early reported [10,21–24]. PyRx-virtual screening tool was utilized to dock all synthetic compounds 2-6 against the target enzyme. The 2D and 3D docking pose images of molecules with the target enzyme were visualized using Discovery studio 3.5 client.

Conclusion

In conclusion, a series of new pyrazole-linked pyran molecules was prepared starting from 4-acetyl-1,3-diphenyl-1H-pyrazole-5(4H)-ole **1**. The structures of the prepared hybrid molecules were proved using spectroscopic techniques. All the prepared molecules were screened for their *in vitro* anti-inflammatory potency. In addition, the docking approach was performed for these molecules. Among these derivatives, compound **6** showed observed anti-inflammatory activity compared with diclofenac.

References

- [1] D. Kumar, P. Sharma, H. Singh, K. Nepali, G.K. Gupta, S.K. Jain, F. Ntie-Kang, The value of pyrans as anticancer scaffolds in medicinal chemistry, RSC Adv. 7 (2017) 36977–36999. <https://doi.org/10.1039/c7ra05441f>.
- [2] M.I. Kadhim, I. Husein, Pharmaceutical and Biological Application of New Synthetic Compounds of Pyranone, Pyridine, Pyrimidine, Pyrazole and Isoxazole Incorporating on 2-Flouroquinoline Moieties, Syst. Rev. Pharm. 11 (2020) 679–684. <https://doi.org/10.5530/srp.2020.2.98>.
- [3] Mohamed Abdel-Rady, Mahmoud H. Mahross, Abu-Bakr A. El-Adasy, Ahmed A. Atalla, Ahmed A. Khames, Abdel Haleem M. Hussein, Functionally substituted arylhydrazones as building blocks in heterocyclic synthesis: Facile synthesis of pyrazoles, triazoles, triazines and quantum chemical studies, Synth. Commun. 51 (2021) 3099–3115. <https://doi.org/10.1080/00397911.2021.1961275>.

- [4] S. Maddila, N. Kerru, S.B. Jonnalagadda, Recent Progress in the Multicomponent Synthesis of Pyran Derivatives by Sustainable Catalysts under Green Conditions, *Molecules* 27 (2022) 1–32. <https://doi.org/10.3390/molecules27196347>.
- [5] H.R.M. Rashdan, A.H. Abdelmonsef, Towards Covid-19 TMRSS2 enzyme inhibitors and antimicrobial agents: Synthesis, antimicrobial potency, molecular docking, and drug-likeness prediction of thiadiazole-triazole hybrids, *J. Mol. Struct.* 1268 (2022) 133659. <https://doi.org/10.1016/j.molstruc.2022.133659>.
- [6] M.A.M. Abdel Reheim, I.S. Abdel Hafiz, H.M. Reffat, H.S. Abdel Rady, I.A. Shehadi, H.R.M. Rashdan, A. Hassan, A.H. Abdelmonsef, New 1,3-diphenyl-1H-pyrazol-5-ols as anti-methicillin resistant *Staphylococcus aureus* agents: Synthesis, antimicrobial evaluation and in silico studies, *Heliyon* 10 (2024) e33160. <https://doi.org/10.1016/j.heliyon.2024.e33160>.
- [7] M. El-Naggar, H.R.M. Rashdan, A.H. Abdelmonsef, Cyclization of Chalcone Derivatives: Design, Synthesis, In Silico Docking Study, and Biological Evaluation of New Quinazolin-2,4-diones Incorporating Five-, Six-, and Seven-Membered Ring Moieties as Potent Antibacterial Inhibitors, *ACS Omega* 8 (2023) 27216–27230. <https://doi.org/10.1021/acsomega.3c02478>.
- [8] S. Akhramez, A. Oumessaoud, A. Hibot, S. Talbi, S. Hamri, E.M. Ketatni, H. Ouchetto, A. Hafid, H. Ayad, N. El Abbadi, C. Zanane, H. Latrache, M. Khouili, M.D. Pujol, Synthesis of pyrazolo-enaminones, bipyrazoles and pyrazolopyrimidines and evaluation of antioxidant and antimicrobial properties, *Arab. J. Chem.* 15 (2022) 103527. <https://doi.org/10.1016/j.arabjc.2021.103527>.
- [9] K.D. Dwivedi, B. Borah, L.R. Chowhan, Ligand Free One-Pot Synthesis of Pyrano[2,3-c]pyrazoles in Water Extract of Banana Peel (WEB): A Green Chemistry Approach, *Front. Chem.* 7 (2020) 1–8. <https://doi.org/10.3389/fchem.2019.00944>.
- [10] A.H. Abdelmonsef, M.E. Mohamed, M. El-naggar, Novel Quinazolin-2, 4-Dione Hybrid Molecules as Possible Inhibitors Against Malaria: Synthesis and in silico Molecular Docking Studies, *7* (2020) 1–19. <https://doi.org/10.3389/fmolb.2020.00105>.
- [11] M.G. Badrey, S.M. Gomha, A.H. Abdelmonsef, A.A.M. El-Reedy, Syntheses and Molecular Docking Analysis of Some New Thiazole and Thiazine Derivatives as Three Armed Molecules with a Triazine Ring as a Core Component: A Search for anti-Obesity Agents, *Polycycl. Aromat. Compd.* 0 (2023) 1–19. <https://doi.org/10.1080/10406638.2023.2173617>.
- [12] R. M. Kassab, M. E. A. Zaki, S. A. Al-Hussain, A. H. Abdelmonsef, Z. A. Muhammad, Two Novel Regioisomeric Series of Bis-pyrazolines: Synthesis, In Silico Study, DFT Calculations, and Comparative Antibacterial Potency Profile against Drug-Resistant Bacteria; MSSA, MRSA, and VRSA, *ACS Omega* 9 (2024) 3349–3362. <https://doi.org/10.1021/acsomega.3c06348>.
- [13] H.R.M. Rashdan, A.H. Abdelmonsef, In silico study to identify novel potential thiadiazole-based molecules as anti-Covid-19 candidates by hierarchical virtual screening and molecular dynamics simulations, *Struct. Chem.* 33 (2022) 1727–1739. <https://doi.org/10.1007/s11224-022-01985-1>.
- [14] R.M. Mohareb, N.Y. MegallyAbdo, Uses of 3-(2-Bromoacetyl)-2H-chromen-2-one in the synthesis of heterocyclic compounds incorporating coumarin: Synthesis, characterization and cytotoxicity, *Molecules* 20 (2015) 11535–11553. <https://doi.org/10.3390/molecules200611535>.
- [15] A.H. Abdelmonsef, M.A. Abdelhakeem, A.M. Mosallam, H. Temairk, M. El-Naggar, H. Okasha, H.R.M. Rashdan, A search for antiinflammatory therapies: Synthesis, in silico investigation of the mode of action, and in vitro analyses of new quinazolin-2,4-dione derivatives targeting phosphodiesterase-4 enzyme, *J. Heterocycl. Chem.* 59 (2022) 474–492. <https://doi.org/10.1002/jhet.4395>.
- [16] S. Yesmin, A. Paul, T. Naz, A.B.M.A. Rahman, S.F. Akhter, M.I.I. Wahed, T. Bin Emran, S.A. Siddiqui, Membrane stabilization as a mechanism of the anti-inflammatory activity of ethanolic root extract of Choi (Piper chaba), *Clin. Phytoscience* 6 (2020). <https://doi.org/10.1186/s40816-020-00207-7>.
- [17] Waheed-Uz-Zuman, R. Ayub, A. Dar, J. Anwar, Determination of Diclofenac Sodium in Pharmaceutical Preparations by Computational Image Scanning Densitometry, *J. Chem. Soc. Pakistan* 45 (2023) 237–242. <https://doi.org/10.52568/001248/JCSP/45.03.2023>.
- [18] A. V. Lebedev, N. Paul, J. Yee, V.A. Timoshchuk, J. Shum, K. Miyagi, J. Kellum, R.I. Hogrefe, G. Zon, Hot Start PCR with heat-activatable primers: A novel approach for improved PCR performance, *Nucleic Acids Res.* 36 (2008) 1–18. <https://doi.org/10.1093/nar/gkn575>.
- [19] A.H. Abdelmonsef, M.A. Abdelhakeem, A.M. Mosallam, H. Temairk, M. El-Naggar, H. Okasha, H.R.M. Rashdan, A search for antiinflammatory therapies: Synthesis, in silico investigation of the mode of action, and in vitro analyses of new quinazolin-2,4-dione derivatives targeting phosphodiesterase-4 enzyme, *J. Heterocycl. Chem.* 59 (2022) 474–492. <https://doi.org/10.1002/jhet.4395>.
- [20] H.R.M. Rashdan, H. Okasha, M.A. Abdelhakeem, A.M. Mosallam, H. Temairk, A.G. Alhamzani, M.M. Abou-Krishna, T.A. Yousef, A.H. Abdelmonsef, Synthesis and In-vitro Biological Analyses of New quinazolin-2,4-dione Derivatives, *Egypt. J. Chem.* 65 (2022) 189–199. <https://doi.org/10.21608/EJCHEM.2022.111820.5077>.
- [21] S.M. Gomha, H.A. Abdelhady, D.Z. Hassain, A.H. Abdelmonsef, M. El-Naggar, M.M. Elaasser, H.K. Mahmoud, Thiazole-Based Thiosemicarbazones: Synthesis, Cytotoxicity Evaluation and Molecular Docking Study, *Drug Des. Devel. Ther.* Volume 15 (2021) 659–677. <https://doi.org/10.2147/DDDT.S291579>.
- [22] A.H. Abdelmonsef, M. Omar, H.R.M. Rashdan, M.M. Taha, A.M. Abobakr, Synthesis, characterization, computer-aided docking studies, and anti-fungal activity of two-armed quinazolin-2,4-dione derivatives, *J. Mol. Struct.* 1316 (2024). <https://doi.org/10.1016/j.molstruc.2024.138854>.
- [23] A.O.A. Ibrahim, A. Hassan, A.M. Mosallam, A. Khodairy, H.R.M. Rashdan, A.H. Abdelmonsef, New quinazolin-2,4-dione derivatives incorporating acylthiourea, pyrazole and/or oxazole moieties as antibacterial agents via DNA gyrase inhibition, *RSC Adv.* 14 (2024) 17158–17169. <https://doi.org/10.1039/D4RA02960G>.

- [24] A.H. Abdelmonsef, A.M. El-Saghier, A.M. Kadry, Ultrasound-assisted green synthesis of triazole-based azomethine/thiazolidin-4-one hybrid inhibitors for cancer therapy through targeting dysregulation signatures of some Rab proteins, *Green Chem. Lett. Rev.* 16 (2023) 2150394. <https://doi.org/10.1080/17518253.2022.2150394>.